Journal of Materials Chemistry A

Accepted Manuscript

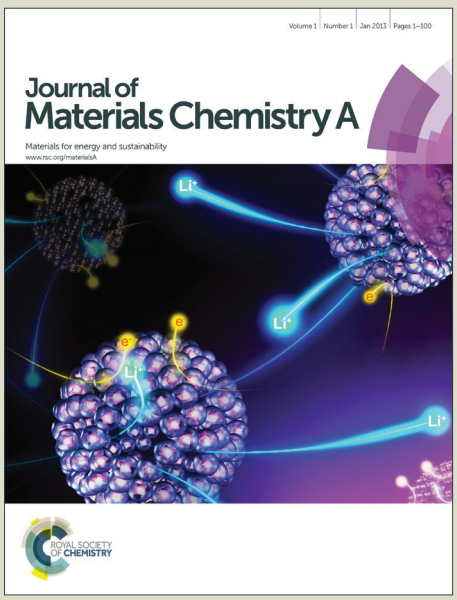

ROYAL SOCIETY OF CHEMISTRY

www.rsc.org/materialsA

Journal of Materials Chemistry A

Dynamic Article Links ►

Cite this: DOI: 10.1039/c0xx00000x

www.rsc.org/xxxxxx

PAPER

One Pot Synthesis of Ultrasmall MoO_3 Nanoparticles Supported on SiO_2, TiO_2, and ZrO_2 Nanospheres: An Efficient Epoxidation Catalyst

Prakash Chandra,[a] Dhananjay S. Doke,[a] Shubhangi B. Umbarkar,[a,b] and Ankush V. Biradar[a,b*]

DOI: 10.1039/b000000x

Ultrasmall molybdenum oxide (MoO_3) nanoparticles supported on various (SiO_2, TiO_2 or ZrO_2) nanospheres were synthesized in one pot using reverse micelle method. The prepared catalysts were extensively characterized by various physico-chemical methods. TEM images showed uniform dispersion of MoO_3 nanoparticles (1.5-4 nm) onto silica (~275 nm). No separate MoO_3 particles were identified from TEM for MoO_3/TiO_2 (~10.5 nm) and MoO_3/ZrO_2 (~6.5 nm) because AHM reacted with titanium and zirconium hydroxides forming solid solution. Among prepared catalysts MoO_3/SiO_2 showed excellent catalytic activity (up to 90% conversion and 100% epoxide selectivity) for olefine epoxidation. The catalyst was successfully recycled up to five cycles without losing much activity and selectivity.

Introduction

The development of environmentally benign technologies have become high priority for the modern chemical industry.[1] For addressing this topic, heterogeneous catalysts have played an important role in development of many processes which includes fuel conversion, pollution abatement and organic transformations.[2] The main focus of the research include the development of effective catalysts that can be easily recovered, reused, and separated from reaction mixtures, making the processes more cost effective and greener. Generally these catalyst consist metals or metal oxides supported on solid supports.[3-4] The presently used industrial catalysts are produced by simple mixing, shaking and baking mixtures of multi-components. Hence their structures and performance relationships are poorly understood. Designing of heterogeneous catalyst involves both the proper control of the surface chemistry and a rigorous control of the surface geometry.[5] The many synthetic methodologies were employed such as atomic layer deposition (ALD)[6], dendrimer encapsulation,[7] sol-gel synthesis,[8] core-shell, york-shell,[9] immobilization procedures, colloidal and reverse micelle[10] etc. for the synthesis of heterogeneous catalyst and used in many organic transformations such as hydrogenation, C-C bond formation and oxidation reactions.

Among all catalytic reactions, oxidation reactions were attracted more attention due to requirement of harsh reaction conditions and selectivity issues.[11] Within various oxidation reactions, olefin epoxidation has been studied extensively as via this process variety of commodity chemicals such as drug intermediates, agrochemicals and food additives can be produced.[12-13] The various homogeneous transition metal complexes and heterogeneous catalyst are known for this reaction.[14] Among known oxidation catalysts molybdenum based catalyst have shown promising activity because it has low oxidation potential and high Lewis acidity in highest oxidation state.[15] Newmann et al.[16] have used MoO_3/SiO_2 for epoxidation of olefins using TBHP as an oxidant. Also Arnold et al.[17] used acid catalyzed sol-gel synthesis of MoO_3/SiO_2 taking Mo(V)-isopropoxide as molybdena precursor for olefin epoxidation. However, both the catalyst show leaching of the active species after three recycles. Supported metal nanoparticles are widely employed in catalysis.[18] Recent advances in controlling the shape and size of nanoparticles have opened the possibility to optimize the particle geometry for enhanced catalytic activity, providing the optimum size and surface properties for specific applications.[19] It has become evident from latest advancement and publications in the field seasonableness of being "green and nano" for nanomaterials synthesis. However, there are very few reports in the literature for synthesis of molybdena nanoparticles and it's catalytic activity. For instance Hyeon et al.[20] have synthesized efficiently recyclable and magnetically separable MoO_x/SiO_2 nanospheres as an efficient olefin epoxidation catalyst. Zeng et al.[21] synthesized MoO_3/SiO_2 mesoporous core@shell and hollow core@shell using *inside-out*

Notes and references

[a] *Catalysis Division, CSIR-National Chemical Laboratory, Dr. Homi Bhabha Road, Pune, 411008, India.*
[b] *Academy of Scientific and Innovative Research, CSIR, Anusandhan Bhawan, New Delhi-110 001, India*
*Corresponding Author: Tel fax: 020 2590 2633.
E-mail: av.biradar@ncl.res.in
† Electronic Supplementary Information (ESI) available: See DOI: 10.1039/b000000x/

preinstallation infusion-hydration method for Fridel-Craft alkylation. Wang et al.[10] have synthesized MoO_3/SiO_2 nanoparticles by reverse micelle or "rasin burn" method for glycerol acetalization with ethylene glycol.

It is well known that MoO_3 supported on silica is an excellent solid acid catalyst for various organic transformations.[22] However their oxygen transfer properties at nano scale size have not been fully explored for epoxidation reaction. Metal nanoparticles, synthesized by reverse micelle showed narrow and uniform size and distribution.[23] Herein we report the easy synthesis of ultrasmall MoO_3 nanoparticles supported on different nanospheres (SiO_2, TiO_2 and ZrO_2) by reverse micelle microemultion i.e "resin burn" method and its application for olefin epoxidation.

Results and discussion

Reverse micelle microemultions are thermodynamically stable and employs surfactant or co-surfactants, water and organic solvents. Reverse micelle solubilises water and provide optimum conditions for synthesis of small nanoparticles as water droplets in nanometer range.[23] We used this method for synthesis of ultrasmall molybdenum oxide nanoparticles supported on various SiO_2, TiO_2 and ZrO_2 nanospheres in one pot (scheme-1).[10] Brij-35 was dispersed in cyclohexane by stirring at 50 °C. After the formation of homogeneous solution, ammonium heptamolybdate (AHM) solution was added into it, this results into the formation of water in oil (w/o) micro emulation. In this process Brij molecules act as an amhiphilic molecule and water droplet formed act as nanoreactor for synthesis of MoO_3 nanoparticles in the bulk oil phase. To the same reaction mixture ammonia hydroxide solution was added followed by tetraethyl orthosilicate (TEOS) and the reaction mixture was stirred for 2 h. Finally, the emulation was broken by addition of iso-propanol followed by sonication. The final reaction mixture was centrifuged to collect the AHM dispersed on metal oxides nanospheres from the reaction media. Then these spheres were dried at room temperature and then calcined at 500 °C in air to get final MoO_3 nanoparticles supported on silica nanospheres. The final sample was named as MoO_3/SiO_2.

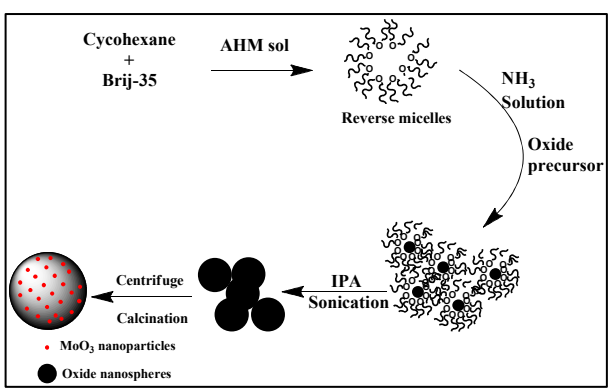

Scheme 1: Schematic representation of the stepwise synthesis of MoO_3/MO_2 (M= Si, Ti or Zr) nanospheres by reverse micelle method.

Similarly, titanium(IV) butoxide and zirconium(IV) butoxide were used as TiO_2 and ZrO_2 precursors for synthesis of MoO_3 nanoparticles supported on TiO_2 and ZrO_2 nanospheres and were named as MoO_3/TiO_2 and MoO_3/ZrO_2 respectively.

The prepared catalysts were fully characterized for their physiochemical properties. The formation of nanospheres and dispersion of MoO_3 nanoparticles on to the oxide support was characterized by transmission electron microscopy (TEM) (fig. 1). In case of MoO_3/SiO_2, SiO_2 nanospheres was uniformly in shape with 275 nm in size . The nanospheres synthesized using Brij-35 was far bigger in size than the reported method.[10] Wang et al. used Brij-58 and obtained silica spheres of 23 nm size. The bigger size silica spheres were obtained, which can accommodate not only large number of MoO_3 nanoparticles but also easy to separate from reaction mixture. After careful analysis by HRTEM, the MoO_3 nanoparticles were found to be in the range of 1.5 to 4 nm with average particle size of 2.3 nm having d-spacing of 0.35 nm for (021) plane of α-MoO_3.[25] Also MoO_3 nanoparticles were monodispersed onto the surface of silica nanospheres. SEM elemental mapping of the same samples supported the fact of uniform dispersion of MoO_3 nanoparticles on silica surface (see fig. 2 A). Yellow spots in the fig. 2B represent molybdena nanoparticles on silica surface. Furthermore, the EDAX analysis showed MoO_3 loading to be 12.48 wt%, in the silica nanospheres (See SI fig. S3-1).

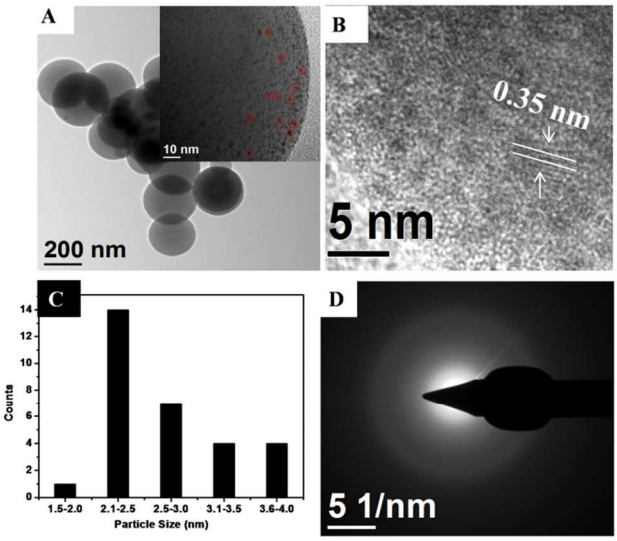

Figure 1: HRTEM image of MoO_3/SiO_2 at (A) 200 nm; inset image shows magnified image at 10 nm; (B) d-spacing of (021) plane of α-MoO_3 nanoparticles on MoO_3/SiO_2 surface. (C) Particle size distributions and (D) SAED pattern of MoO_3/SiO_2.

HRTEM analysis of MoO_3/TiO_2 and MoO_3/ZrO_2 samples (fig. 3 and 4 respectively) showed the formation of uniform size titania and zirconia nanospheres. The size of spheres was about 10.5 nm and 6.5 nm respectively with d-spacing for 0.357 nm for (101) plane of titania[26] and 0.318 nm for (101) plane for tetragonal zirconia.[27] However, MoO_3 nanoparticles

was not identified separately as AHM reacted with titania and zirconia hydroxides forming solid solution in both the samples. Also titania and zirconia nanospheres formed are far smaller than the silica. In the case of TEOS, the alkoxide was more stable, resulting into slower rate of hydrolysis and slower nucleation and crystal growth, and leading to formation of bigger particles in the range of 250 to 300 nm. Whereas in case of zirconia and titana the alkoxide precursor, that is zirconium(IV) butoxide and titanium(IV) butoxide are less stable, resulting in fast hydrolysis and nucleation, and formed smaller nanoparticles in the range of 10 to 20 nm. EDAX analysis

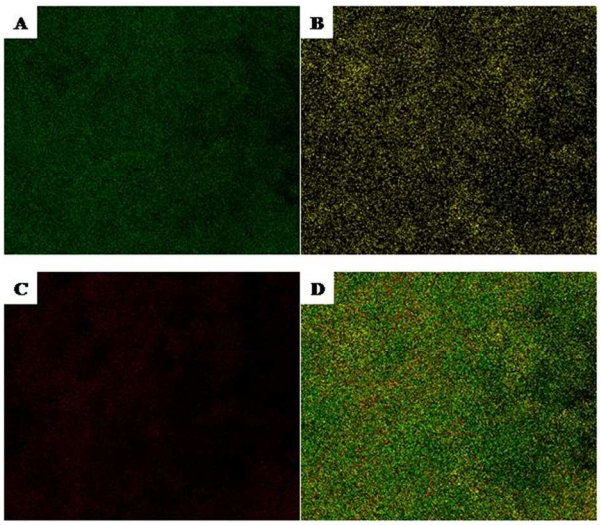

Figure 2: SEM elemental mapping of the MoO_3/SiO_2 surface; (A) green color shows Si content; (B) yellow color shows molybdena atoms; (C) red colors represents oxygen atoms present on surface and (D) MoO_3/SiO_2.

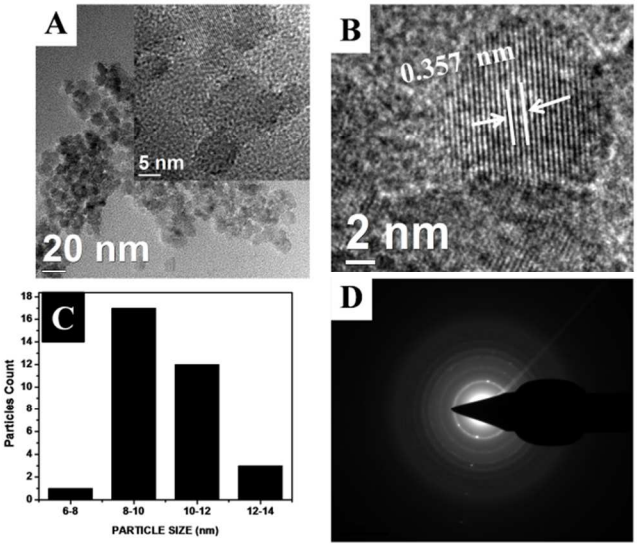

Figure 3: HRTEM image of MoO_3/TiO_2 at (A) 20 nm; inset image shows magnified image at 5 nm; (B) d-spacing for MoO_3/TiO_2 nanoparticles at 101 plane; (C) Particle size distributions and; (D) SAED pattern of MoO_3/TiO_2.

revealed that MoO_3 content was 9.85% and 9.57% of zirconia and titania nanospheres respectively (See SI fig. S3-2-5).

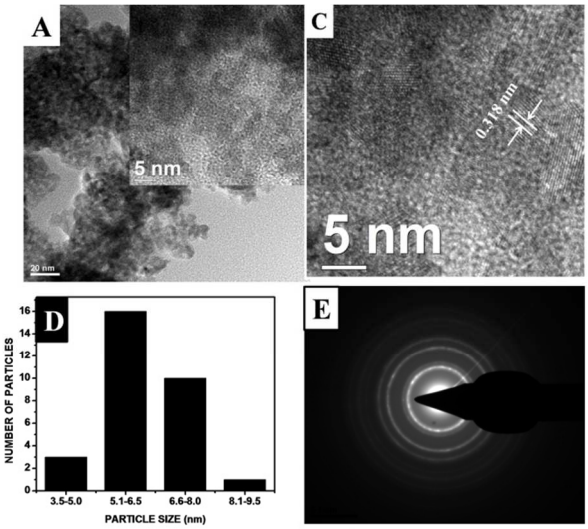

Figure 4: HRTEM image of MoO_3/ZrO_2 at (A) 20 nm; inset image shows magnified image at 5 nm; (B) d-spacing for (101) plane of tetragonal ZrO_2; (C) Particle size distributions and (D) SAED pattern of MoO_3/ZrO_2.

The crystallinity and phase purity was examined by powder X-ray diffraction (fig.-5). The MoO_3/SiO_2 showed the sharp Bragg reflection peaks at 2θ = 12.7 (020), 23.4 (110), 25.7 (040) and 27.4° (021) characteristic of α-MoO_3 orthorhombic phase with crystalline nature (JCPDS No. 05-0508).[22a, 25] These results are comparable to reported literature.[10] The bulk structure of pure ZrO_2 and supported MoO_3/ZrO_2 was determined by X-ray diffraction. Four diffraction peaks in the 2θ range of 20-40° were detected at 24.2, 28.3, 31.3, and 34.3 with a shoulder at 35.4°. These can be attributed to monoclinic ZrO_2 structures (JCPDS card no. 37-1484) (See SI fig. S3-1). However in case of MoO_3/ZrO_2 nanospheres, the XRD pattern showed broad peaks at 2θ = 30.3, 35.3, 50.4 and 60° indicating the formation of exclusively tetragonal zirconia phase. Appearance of peaks around 30.3, 35.3, 50.4° indicated the formation of $Zr(MoO_4)_2$ species and confirmed presence of strong interaction between molybdena and zirconia.[26-30] Hence no separate MoO_3 diffractions lines were observed. MoO_3/TiO_2 showed characteristic peaks for anatase TiO_2 phase (JCPDS No. 21-1272).[31] No peaks corresponding to MoO_3 were observed indicating presence of very tiny and well dispersed molybdenum oxide particles on titania surface. In case of MoO_3/SiO_2, the MoO_3 nanoparticles formed during the Brij interactions get dispersed on silica nanospheres and formed bulk MoO_3 which was seen in XRD. In case of MoO_3/TiO_2 and MoO_3/ZrO_2 system MoO_3 nanoparticles initially formed with Brij treatment reacted with titanium and zirconium hydroxides forming solid solutions with TiO_2 and ZrO_2, and uniformly dispersed as amorphous MoO_3 nanoparticles were not seen as bulk crystalline MoO_3 in XRD.

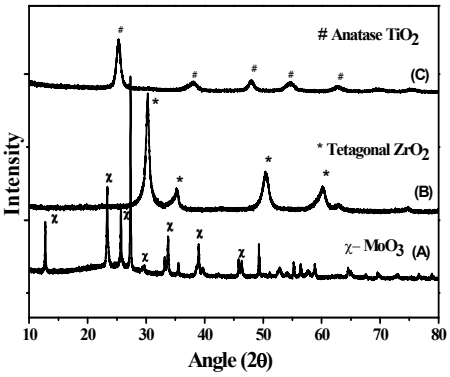

Figure 5: Powder XRD pattern of MoO_3 nanoparticles supported on (A) Silica; (B) Zirconia and (C) Titania nanospheres.

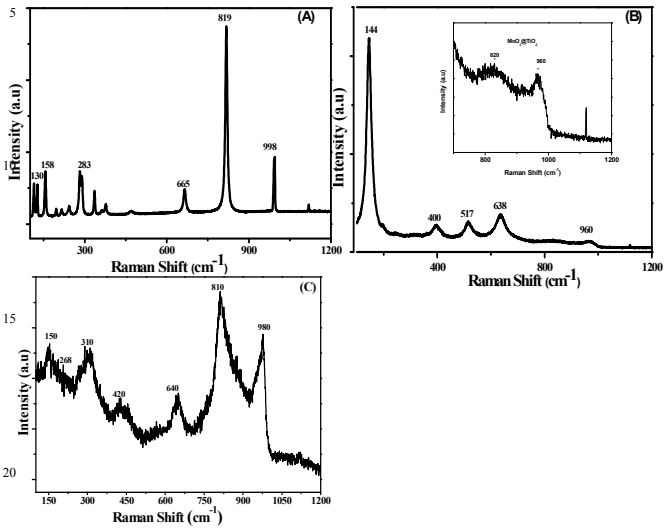

Figure 6: Raman spectra of (A) MoO_3/SiO_2; (B) MoO_3/TiO_2; inset graph shows expanded view in range the 700 - 1200 cm^{-1} and (C) MoO_3/ZrO_2.

The structure of molybdena supported on oxides was examined using Raman spectroscopy (fig.-6). The Raman spectrum of MoO_3/SiO_2 (fig.-6A) showed bands around 998 cm^{-1} due to terminal M=O stretching mode. The band around 819 cm^{-1} was due to bulk MoO_3 species. A small and broad band in the range 660 cm^{-1} and 270-280 cm^{-1} was due to Mo-O-Mo stretching and deformation respectively.[17, 23] The expected weak bridging Mo-O-Si band was not readily observed in the 900–930 cm^{-1} region. Remaining bands were in agreement with α-MoO_3 species present on the SiO_2 surface.[32] Raman spectrum of MoO_3/TiO_2 clearly showed the formation of anatase phase, due to the appearance of bands in the region 144, 400, 517 and 638 cm^{-1}. A broad band around 960 cm^{-1} clearly represented the formation of well dispersed MoO_3 species on the titania surface. Raman spectrum of MoO_3/ZrO_2 showed tetragonal ZrO_2 at 150, 268, 310, 420, 600 (shoulder), and 640 cm^{-1}. The bands around 810 cm^{-1} and 980 cm^{-1} were due to Mo-O-Mo vibrations and Mo=O stretching frequencies respectively. Tetragonal ZrO_2 showed bands at 150, 268, 310, 420, 600 (shoulder), and 640 cm^{-1}. The bands around 810 cm^{-1} and 980 cm^{-1} were due to Mo-O-Mo vibrations and Mo=O stretching frequency respectively.[31, 33-36,]

The quantitative analysis of Mo=O to Mo-O-Mo content present in molybdena supported on oxide support following formula was employed.[36]

$$fm = \sqrt{0.19 - \frac{0.13}{Xm - 1.01}} - 0.56 \qquad (1)$$

Here $X_m = I_{Mo=O} / \{I_{Mo=O} + I_{Mo\text{-}O\text{-}Mo}\}$, m is Mo=O or Mo-O-Mo and fm represents the Mo=O or Mo-O-Mo contents present in catalyst. The Mo-O-Mo/Mo ratio for MoO_3/SiO_2 was 6.5, MoO_3/ZrO_2 was 1.31 and MoO_3/TiO_2 was 1.14.

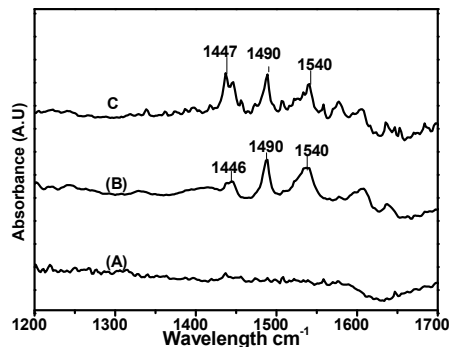

Figure 7: FTIR of adsorbed pyridine on (A) MoO_3/SiO_2; (B) MoO_3/TiO_2 and (C) MoO_3/ZrO_2 at 100 °C.

The presence of Lewis and Brönsted acidic sites was determined by FTIR of adsorption of pyridine.[37-38] When pyridine was adsorbed on the MoO_3/SiO_2 samples then adsorption bands for either Lewis or Brönsted acidity was not found. This indicates that either very weak or no acidity is present on the sample. Furthermore, MoO_3/TiO_2 showed bands around 1447 cm^{-1} due to Lewis acid sites 1540 cm^{-1} confirmed presence of Brönsted acidity. MoO_3/ZrO_2 also showed presence of Lewis and Brönsted acidic sites on MoO_3/TiO_2.

To determine total acidity and the acid strength of the molybdena nanoparticles dispersed on various oxide nanospheres, NH_3-temperature programmed desorption (TPD) was carried out. MoO_3/SiO_2, MoO_3/TiO_2 and MoO_3/ZrO_2 (Fig S-7 (A), (B) and (C)) showed one signal below 500 °C. Total acidity of the all the supported molybdena catalysts was in the order MoO_3/TiO_2 (0.45 mmol/g) ≈ MoO_3/ZrO_2 (0.45 mmol/g) > MoO_3/SiO_2 (0.196 mmol/g).

XPS analysis was performed in order to obtain the elemental composition, chemical and electronic state of molybdena on oxide support. All the binding energies were calibrated using the C 1s peak at 284.6 eV. XPS analysis of MoO_3/SiO_2 showed peak at 232.7 eV and 235.9 eV due to Mo $3d_{5/2}$ and Mo $3d_{3/2}$, respectively. The single peak of Si 2p with binding energy of 102.8 eV corresponds to the binding state of Si in SiO_2 (See SI fig. S6-1). In case of MoO_3/TiO_2 molybdenum 3d showed peaks of $3d_{5/2}$ and $3d_{3/2}$ at 232.9 eV and 235.9 eV. Peaks around 458.9 eV and 464.5 eV were due to the Ti $2p_{3/2}$ and Ti $2p_{1/2}$. (See SI

fig. S8-2) XPS spectra of MoO_3/ZrO_2 showed peak at 232.9 eV and 235.9 eV due to Mo3d $_{5/2}$ and Mo 3d $_{3/2}$ present in MoO_3. Zr 3d $_{5/2}$ and Zr 3d $_{3/2}$ showed peaks at 182.6 eV and 184.9 eV.

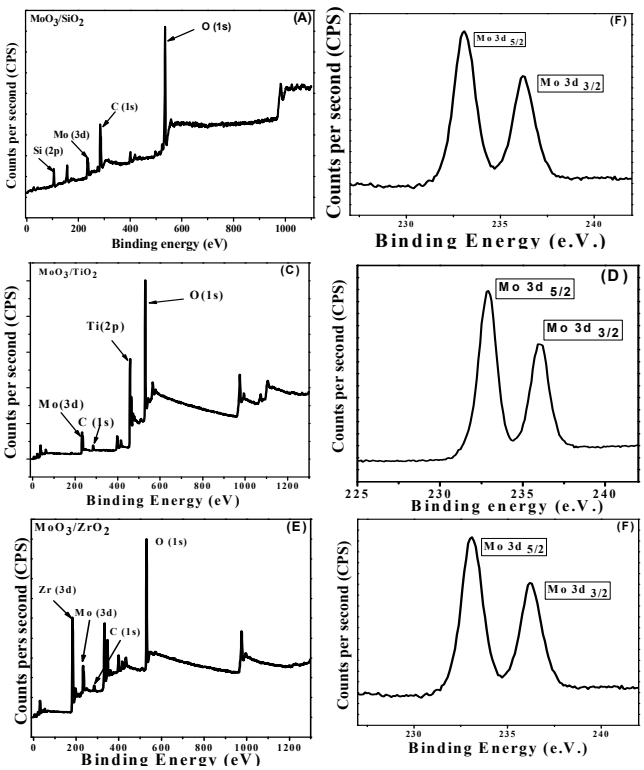

Figure 8: XPS spectra of (A) MoO_3/SiO_2; (B) Mo present in MoO_3/SiO_2, (C) MoO_3/TiO_2; (D) Mo present in MoO_3/TiO_2 (E) MoO_3/ZrO_2; (F) Mo present in MoO_3/ZrO_2.

The Brunauer–Emmett–Teller (BET) surface area and pore diameters of the molybdena on different oxide supports was determined by N_2 adsorption measurements (See SI fig. S6-1). All the samples showed a type-IV isotherm and the presence of mesoporosity on the catalyst surface having pore diameter in the range 20 to 500 Å. Surface area of MoO_3/SiO_2 was found to be 22.8 m^2/g. The total pore volume and average pore diameter were found to be 0.009982 cc/g and 33.4950 Å. whereas surface area of MoO_3/TiO_2 was found to be 89.1 m^2/g. The total pore volume was 0.09281 cc/g and average pore diameter was 20.8203 Å. MoO_3/ZrO_2 had surface area of 139.6 m^2/g with total pore volume and average pore diameter were found to be 0.2494 cc/g and 34.7939 Å respectively. The surface area of the materials decreased in the order $MoO_3/ZrO_2 > MoO_3/TiO_2 > MoO_3/SiO_2$.

Catalytic reactions

The catalytic activity of the prepared MoO_3 nanoparticles supported on different nanospheres was tested by selecting cyclooctene as a probe reactant and TBHP as an oxidant (scheme-2). First, the reaction was carried out without catalyst to check the oxidation capabilities of the oxidant (TBHP) itself. It was observed that only 12% cyclooctene conversion was obtained after stirring the reaction mixture at 80 °C for 2 h, and cyclooctene epoxide was obtained as the sole product (Table 1 entry 1). This could be the autocatalysis by thermal reaction.

Scheme 2: Epoxidation of cyclooctene.

Table 1: Results of epoxidation of cyclooctene using MoO_3 nanoparticles dispersed onto the different nanospheres as catalysts[a]

Entry	Catalsyt	% Conv.	% Epoxide Sel.	TOF h^{-1}[#]
1.	Blank[b]	12	100	-
2.	MoO_3/SiO_2	90	100	72.3
3.	MoO_3/TiO_2	37	100	24.8
4.	MoO_3/ZrO_2	39.6	100	25.9

[a]**Reaction condition:** Cyclooctene: 0.282 g (0.0025 mol); Oxidant: 5.5 molar TBHP in decane (0.0025 mol); Catalyst: 0.028 g; Temperature: 80 °C; Solvent: 1, 2-dichloroethane (6 g); Time-2 h; [b]: Without catalyst. [#] TOF calculated after 2 h.

When MoO_3/SiO_2 was used as catalyst and 1:1 substrate to oxidant ratio, it gave 90% cyclooctene conversion and 100% selectivity to cyclooctene epoxide within 2 h reaction time with TOF of 72.3 h^{-1}. Furthermore, MoO_3 nanoparticles supported on both zirconia and titania nanospheres were used as catalyst under same reaction condition. MoO_3/TiO_2 as a catalyst gave 37% conversion of cycloocetene with 100% selectivity for epoxide. Also when used MoO_3/ZrO_2 catalyst which gave only 39.6% conversion of cyclooctene in 2 h, and 100% epoxide selectivity. These results clearly indicated that MoO_3/SiO_2 nanospheres gave the best results for considering the catalytic oxidation of cyclooctene. The higher activity may be attributed to the presence of large number of MoO_3 oxide nano particles uniformly dispersed on the surface of silica nanospheres (Mo-O-Mo/Mo=O value was highest (6.5)) which favored high olefin epoxidation and which is very less in the case of ZrO_2 and TiO_2.

Furthermore, we studied the substrate scope by selecting other olefins and MoO_3/SiO_2 nanospheres as catalyst. When cyclooctene was used as substrate, it gave very high conversion and selectivity for epoxides (Table 2 entry 1). When cyclooctadiene was oxidized it gave complete conversion with mono and di- epoxide as products (Table 2 entry 3). However cyclohexene gave poor conversion in 2 h (Table 2 entry 2). Further extending the reaction time it gave 90% conversion in 6 h. with 90% selectivity for epoxide. Cyclohexadiene as substrates gave 70% conversion and 58% and 42% selectivity to mono and di epoxide. Under similar condition styrene gave 47% conversion with 67% selectivity for epoxide and 37% for benzaldehyde as product.

Table 2: Results of epoxidation of other olefins using MoO_3/SiO_2 nanospheres as a catalyst[a]

Entry	Substrates	% Conv.	% Epoxide Sel.	TOF $h^{-1\#}$
1.		90	100	72.3
2.		44 90[@]	100 90	49.5
3.		74	85.3, 14.6[*]	61.7
4.		70	58.3, 41.7[$]	78.7
5.	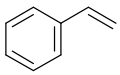	47	67 , 33[β]	10.2

[a]**Reaction condition:** Substrates: 0.0025 mol; Oxidant: 5.5 molar TBHP in decane (0.0025 mol); Catalyst (MoO_3/SiO_2 nanospheres): 10 wt% of substrates; Temperature: 80 °C; Solvent: 1, 2-dichloroethane (6 g); Time-2 h; [#] TOF calculated after 2 h.[@] 6h reaction time, * 5,10-dioxatricyclo[7.1.0.04,6]decane;$ 3,8dioxatricyclo[5.1.0.02,4]octane; [β] benzaldehyde

The best catalyst i.e. MoO_3/SiO_2 nanospheres was used to check the reusability for epoxidation reaction. After each reaction cycle the catalyst was separated by centrifugation and washed with solvent and used for next run. There was no considerable decrease in conversion and epoxide was found even after five cycles. (See SI fig. S9). TEM investigations of catalyst after 5th recycle showed no change in shape and size of MoO_3 and silica nanospheres (See SI fig S10). Particle size after fifth cycle was found to be around 2.5 nm which was similar to the fresh catalyst. Leaching test was carried out using hot filtration experiment and results are shown in (See SI fig. S11). After 1h, the reaction was stopped and catalyst was removed from reaction media by centrifugation and supernant was allowed to react further without catalyst. It gave only additional 12% conversion in 1h. which may be due to thermal reaction catalysed by TBHP, as shown in blank reaction.[39] This indicated that the reaction was truly catalyzed by MoO_3 nanoparticles supported onto the surface of silica nanospheres.

These results are in line or better the reported methods, for instance Arnold et *al.*[17] used acid catalysed sol-gel synthesis of MoO_3/SiO_2 taking Mo(V)-isopropoxide as molybdena precursor for olefin epoxidation. Cyclohexene oxidation was carried out using TBHP as oxidant gave 94% conversion, with 96% epoxide selectivity in 8 h with TOF as high as 229. But catalyst showed poor recyclability after three recycles and molybdena leached out from catalyst surface. Bakala and co-workers have reported the olefin epoxidation using molybdena supported on mesoporous silica (MCM-41, SBA-15). TBHP was taken as oxidant in a molar ratio three times as compared to the cyclooctene. They obtained 97% conversion and 95% epoxide selectivity using decane as solvent at 40 °C in 3 h.[40] However, both the catalysts showed leaching of the active species after three recycles.

Conclusions

Reverse micelle micro-emulsion was proved to be efficient method for the synthesis of ultrasmall molybdenum oxide nanoparticles with definite structure and uniform distribution over the SiO_2, TiO_2 and ZrO_2 nanospheres. These MoO_3 nanoparticles were found to be excellent olefin epoxidation catalysts and gave exclusive epoxide products. The particles size of MoO_3 does not seem to be very important for conversion and selectivity. Catalyst was recyclable up to five cycles without any loss of catalytic activity or leaching of metal oxide nanoparticles from catalyst surface.

Materials and method

All the reagents viz., ammonium heptamolybdate (Thomas Baker), Cyclooctene, 1,4 dicyclopentadiene, cyclohexene, 1, 3 dicyclohexene, n-hexene, 5.5M TBHP in decane, *tetra*-ethylorthosilicate (TEOS), titanium (IV) butoxide (Aldrich), zirconia (IV) butaoxide (Aldrich), isopropyl alcohol, polyoxyethylene(23) lauryl ether (Brij-35) (Thomas Baker) and 1,2-dichloroethane (S.D. fine chemicals) were used as received.

Synthesis of MoO_3/SiO_2: In a typical synthesis, 250 mL two necked round-bottom flask was charged with 2.42 g Brij-35 (3 mmol) and 60 mL cyclohexane. The flask was stirred at 50 °C for 30 min or until complete dissolution of Brij-35. Then 2 mL ammoniumheptamolybdate solution (0.1M) was added and reaction mixture was stirred for 1 h. After this 2 mL distilled water and 4.8 mL ammonium hydroxide was added slowly and again stirred for 15 min. To this solution, 4 g TEOS was added slowly and allowed to stir for additional 2 h. The reaction was quenched by addition of 40 mL isopropanol followed by ultrasonication for 5 min. The final AHM on SiO_2 nanospheres were collected by centrifugation (5000 rpm for 10 min). The precipitate was washed with IPA and methanol (40 mL) and dried at room temperature and then calcined at 500 °C for 5 h under air to get MoO_3/SiO_2 nanospheres.

Synthesis of MoO_3/TiO_2: For the synthesis of MoO_3/TiO_2, the similar procedure was followed as above, only 5.2 g titanium(IV) butoxide was used as metal oxide precursor instead of TEOS and catalyst was named as MoO_3/TiO_2 nanospheres.

Synthesis of MoO_3/ZrO_2: For the synthesis of MoO_3/ZrO_2, the similar procedure was followed as above, only 4 g zirconium(IV) butoxide was used as metal oxide precursor instead of TEOS and catalyst was named as MoO_3/ZrO_2 nanospheres.

Catalyst characterization: All the catalysts were characterized by various physicochemical techniques and details of instruments and methods are given in supplementary information S1.

Typical reaction procedure: The liquid phase catalytic oxidation was carried out in a 25 mL two necked round bottom flask equipped with a magnetic stirrer and immersed in a thermostat oil bath. The flask was charged with cyclooctene (0.0025 mol), oxidant (0.0025 mol) 5.5 M TBHP in decane, 0.02 g catalyst and dichloroethane (6 g) as a solvent. The samples were withdrawn periodically and analysed on Agilent 6890 Gas chromatograph equipped with a HP-5 dimethyl polysiloxane column (60 m length, 0.25 mm diameter and 0.25 µm film thicknesses) with flame ionization detector. Products were confirmed by GC-MS 6890N.

Acknowledgement

PC acknowledges CSIR New Delhi for providing the fellowship, AVB acknowledges Director CSIR-NCL for providing QHS and in-house project MLP 028026. Also Mr. Ketan Bhotkar is acknowledged for help in EDAX analysis.

Refereences

1. P. Tundo, P. Anastas, D. S. Black, J. Breen, T. Collins, S. Memoli, J.Miyamoto, M. Polyakoff, and W. Tumas *Pure Appl. Chem.,* **2000**, *72, (7)*, 1207–1228.
2. a) R**.** A**.** Sheldon, H van Bekkum - Fine chemicals through heterogeneous catalysis **2008** ; b) F. Zaera, *Chem. Soc. Rev.* **2013**, *42*, 2746-2762.
3. D. Astruc, *Nanoparticles and catalysis*, Wiley Online Library, **2008**.
4. R. J. White, R. Luque, V. L. Budarin, J. H. Clark, D. J. Macquarrie, *Chem. Soc. Rev.* **2009**, *38*, 481-494.
5. I. Lee, F. Delbecq, R. Morales, M. A. Albiter F. Zaera *Nat. Mater* **2009**, *8,* 132-138.
6. S. T. Christensen, H. Feng, J. L. Libera, Neng Guo, J. T. Miller,P. C. Stair, J. W. Elam, *Nano Lett.* **2010**, *10*, 3047–3051
7. A. V. Biradar, A. A. Biradar, T. Asefa, *Langmuir* **2011**, *27*, 14408-14418.
8. R. D. Gonzalez, T. Lopez, R. Gomez, *Catal. Today* **1997**, *35*, 293-317.
9. Y. Wang, A. V. Biradar, C. T. Duncan, T. Asefa, *J. Mater. Chem.* **2010**, *20*, 7834-7841.
10. J. Wang, X. Li, S. Zhang, R. Lu, *Nanoscale* **2013**, *5*, 4823-4828.
11. M. Beller, C. Bolm, *Transition Metals for Organic Synthesis: Building Blocks and Fine Chemicals, 2 Volume Set*, Wiley-VCH New York:, **2004**.
12. B. S. Lane, K. Burgess, *Chem. Rev.* **2003**, *103*, 2457-2474.
13. A. K. Yudin, *Aziridines and epoxides in organic synthesis*, John Wiley & Sons, **2006**.
14. K. A. Jørgensen, *Chem. Rev.* **1989**, *89*, 431-458.
15. M. Jia, W. R. Thiel, *Chem. Commun.* **2002**, 2392-2393.
16. D. Juwiler, R. Neumann, J. Blum, *Chem. Commun.* **1998**, 1123-1124.
17. U. Arnold, R. Serpa da Cruz, D. Mandelli, U. Schuchardt, *J. Mol. Catal. A: Chem.* **2001**, *165*, 149-158.
18. G. Prieto, J. Zečević, H. Friedrich, K. P. de Jong & P. E. de Jongh *Nat. Mater.* **2013***, 12*, 34-39.
19. F. Zaera, *Catal. lett.* **2012**, *142*, 501-516.
20. M. Shokouhimehr, Y. Piao, J. Kim, Y. Jang, T. Hyeon, *Angew. Chem.* **2007**, *119*, 7169-7173.
21. J. Dou, H. C. Zeng, *J. Am. Chem.Soc.* **2012**, *134*, 16235-16246.
22. a) T. V. Kotbagi, A. V. Biradar, S. B. Umbarkar, M. K. Dongare, *ChemCatChem* **2013**, *5*, 1531-1537; b)J. Muijsers, T. Weber, R. Vanhardeveld, H. W. Zandbergen, J. Niemantsverdriet, *J. Catalysis* **1995**, *157*, 698-705; c) R. Sheldon, J. Van Doorn, *J. Catal.* **1973**, *31*, 427-437; d) M. A. Banares, H. Hu, I. E. Wachs, *J. Catal.* **1994**, *150*, 407-420; e) N. D. Spencer, *J. Catalysis* **1988**, *109*, 187-197.
23. J. Eastoe, M. J. Hollamby, L. Hudson *Adv. Col. Inter.Sci.* **2006,** *128–130,* 5–15
24. S. Santra, R. Tapec, N. Theodoropoulou, J. Dobson, A. Hebard, W. Tan, *Langmuir* **2001**, *17*, 2900-2906.
25. A. Klinbumrung, T. Thongtem, S. Thongtem, *J. Nanomater.* **2012**, *1-5*,
26. Z. Zhang, X. Zhong, S. Liu, D. Li, M. Han, *Angew. Chem.* **2005**, *117*, 3532-3536.
27. C.-C. Chen, W.-Y. Cheng, S.-Y. Lu, Y.-F. Lin, Y.-J. Hsu, K.-S. Chang, C.-H. Kang, K.-L. Tung, *CrystEngComm* **2010**, *12*, 3664-3669.
28. Z. Liu, Y. Chen, *J. Catal.* **1998**, *177*, 314-324.
29. E. El-Sharkawy, A. Khder, A. Ahmed, *Micro. Meso. Mater.* **2007**, *102*, 128-137.
30. B. Samaranch, P. Ramírez de la Piscina, G. Clet, M. Houalla, N. Homs, *Chem. . Mater.* **2006**, *18*, 1581-1586.
31. T. Kotbagi, D. L. Nguyen, C. Lancelot, C. Lamonier, K. A. Thavornprasert, Z. Wenli, M. Capron, L. J. Duhamel, S. Umbarkar, M. Dongare, *ChemSusChem* **2012**, *5*, 1467-1473.
32. M. Cornac, A. Janin, J. Lavalley, *Polyhedron* **1986**, *5*, 183-186.
33. E. Djurado, P. Bouvier, G. Lucazeau, *J. . Solid State Chem.* **2000**, *149*, 399-407.
35. S. Xie, K. Chen, A. T. Bell, E. Iglesia, *J. Phys. Chem. B* **2000**, *104*, 10059-10068.
36. Z. Liu, L. Dong, W. Ji, Y. Chen, *J. Chem. Soc., Far. Trans.* **1998**, *94*, 1137-1142.
374. M. M. Mohamed, *Appl.Catal.. A, Gen.* **2004**, *267*, 135-142.
38. A. V. Biradar, S. B. Umbarkar, M. K. Dongare, *Appl. Catal. A: Gen.* **2005**, *285*, 190-195.
39. J. Zhang, A. V. Biradar, S. Pramanik, T. J. Emge, T. Asefa, J. Li, *Chem. Commun.* **2012**, *48*, 6541-6543.
40. P. C. Bakala, E. Briot, L. Salles, J.-M. Brégeault, *Appl.Catal.. A, Gen.* **2006**, *300*, 91-99.

One Pot Synthesis of Ultrasmall MoO_3 Nanoparticles Supported on SiO_2, TiO_2, and ZrO_2 Nanospheres: An Efficient Epoxidation Catalyst

Prakash Chandra, Dhananjay S. Doke Shubhangi B. Umbarkar, and Ankush V. Biradar

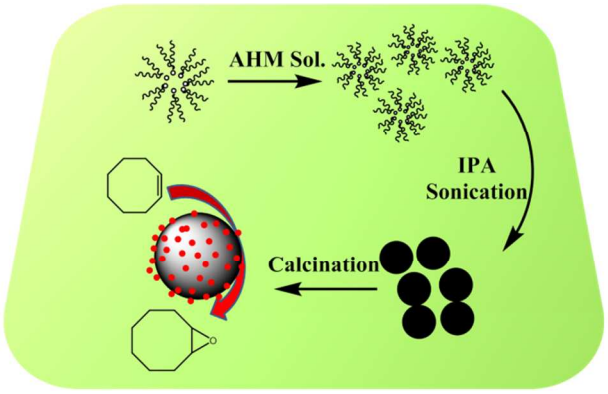

Highlight of work

Utilization of ultrasmall MoO_3 nanoparticles supported on silica nanospheres as a recyclable catalyst in olefin epoxidation